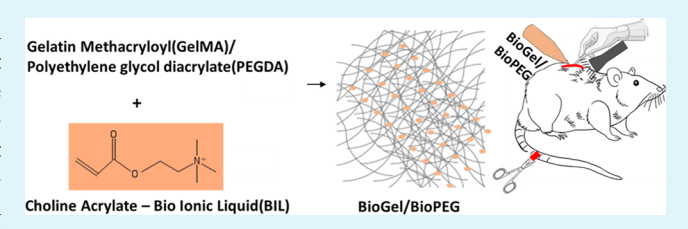


# Bioionic Liquid Conjugation as Universal Approach To Engineer Hemostatic Bioadhesives

Vaishali Krishnadoss, †© Atlee Melillo, \*Baishali Kanjilal, †Tyler Hannah, \*Ethan Ellis, †Andrew Kapetanakis, Joshua Hazelton, Janika San Roman, Arameh Masoumi, Jeroen Leijten, and Iman Noshadi\*,†©

Supporting Information

ABSTRACT: Adhesion to wet and dynamic surfaces is vital for many biomedical applications. However, the development of effective tissue adhesives has been challenged by the required combination of properties, which includes mechanical similarity to the native tissue, high adhesion to wet surfaces, hemostatic properties, biodegradability, high biocompatibility, and ease of use. In this study, we report a novel bioinspired design with bioionic liquid (BIL) conjugated



polymers to engineer multifunctional highly sticky, biodegradable, biocompatible, and hemostatic adhesives. Choline-based BIL is a structural precursor of the phospholipid bilayer in the cell membrane. We show that the conjugation of choline molecules to naturally derived polymers (i.e., gelatin) and synthetic polymers (i.e., polyethylene glycol) significantly increases their adhesive strength and hemostatic properties. Synthetic or natural polymers and BILs were mixed at room temperature and cross-linked via visible light photopolymerization to make hydrogels with tunable mechanical, physical, adhesive, and hemostatic properties. The hydrogel adhesive exhibits a close to 50% decrease in the total blood volume loss in tail cut and liver laceration rat animal models compared to the control. This technology platform for adhesives is expected to have further reaching application vistas from tissue repair to wound dressings and the attachment of flexible electronics.

KEYWORDS: Bioadhesives, Hemostatic, Bioionic liquid, Hydrogels, Traumatic injury

#### 1. INTRODUCTION

Adhesives with the ability to bond to biological tissues have numerous applications including drug delivery, 1,2 tissue repair,<sup>3,4</sup> wound dressings,<sup>5,6</sup> biomedical implants, and flexible wearable electronic devices.<sup>7,8</sup> The primary requirements of adhesive materials for in vivo application are the ability to rapidly stem blood loss and adhere quickly and firmly to the tissue of choice. 9-13 The process of attachment and adhesion to native tissues often is challenged by the wet and dynamic in vivo environment. Adhesive hydrogels are also expected to degrade in a timely fashion and have no cytotoxicity toward the host tissues. Thus, it should accelerate and have no deleterious influence on the healing of the wound. 14-16 Quality, production cost, stability in vivo, and safety are further considerations. <sup>17–19</sup> Moreover, tunable mechanical strength and adhesion of the material are often considered as highly desireable. 20,21

A major limitation of the currently available commercial tissue adhesives is their poor performance due to the low adhesion to wet surfaces and in the environments involving dynamic and cyclic stresses. The lack of adequate flexibility and adhesion is yet another drawback in currently available

commercial adhesives.<sup>22</sup> Cyanoacrylates, for instance, have high adhesive strength but are associated with cytotoxicity and an unnaturally high stiffness. 15,23 Fibrin-based sealants such as fibrin glue are flexible like the soft tissues but only offer weak adhesion strengths, particularly under wet conditions such as those found in tissues.<sup>24</sup>

Despite the commercial availability of adhesives, superior alternatives are wanted, in particular for the repair of elastic and soft tissues in wounded lungs, heart, and blood vessels.<sup>22</sup> Achieving such a formulation demands a material that offers significant adhesion with minimal toxicity and that avoids any damage to tissues arising from the mechanical properties of sealants.<sup>25-34</sup>

In this paper, we report a new adhesive biomaterial platform that offers high adhesion and hemostatic properties under wet conditions, compatible with both synthetic and naturally derived biomaterials, proffering the advantage of a direct bonding mechanism with the lipid bilayer cell membrane

Received: May 24, 2019 Accepted: September 16, 2019 Published: September 16, 2019



<sup>&</sup>lt;sup>†</sup>Department of Chemical Engineering and <sup>‡</sup>Department of Biomedical Engineering, Rowan University, Glassboro, New Jersey 08028-1700, United States

<sup>&</sup>lt;sup>§</sup>Cooper Medical School of Rowan University, Camden, New Jersey 08103-1211, United States

Developmental BioEngineering (DBE), The University of Twente, 7522 NB Enschede, Netherlands

structure, combining high intrinsic mechanical strength with excellent tissue adhesion. This biointeraction inspired platform uses strong coulomb interactions between the polymer structure and the cell membrane's phospholipid bilayer's hydrophilic heads accounting for strong adhesion even in the presence of body fluids and blood. The mechanism of adhesion is feasible for any kind of tissue, not requiring the use of fibrous networks for support, and hence can be used in various applications. This is achieved via the functionalization of polymers—biological or synthetic—with a bioionic liquid (BIL). Ionic liquids are low melting organic salts with high water solubility.<sup>26</sup> Bioionic liquids are a class of ionic liquids where the inorganic counter anions of the ionic liquid structure are replaced by bio-organic molecules, such as the cholinium ion as represented here. 27-29

Ionic liquids may have numerous interesting applications owing to their high thermal stabilities, conductivities, and antimicrobial and antifouling properties. 26,30 Importantly, choline-based biocompatible, noncytotoxic, and biometabolizable ionic liquids are reported. 31,32 Choline is also a structural precursor of the phospholipid cellular membrane bilayer and can help enhance interactions with cell membranes via electrostatic bonding.<sup>33–35</sup> In this paper, we describe a method to conjugate BIL to polymers that are both natural and synthetic to yield bioadhesives. In this study, we assess the conjugation of choline-based BIL to two polymer backbones: a gelatin biopolymer and a synthetic polyethylene glycol diacrylate (PEGDA) polymer. The naturally derived biopolymer used in this study was gelatin methacryloyl (GelMA). The synthesized adhesive exhibits excellent mechanical integrity and tissue adhesion, even in the presence of body fluids, and also superior hemostatic properties. The conjugation of a choline-based BIL allows the polymer to interact with the phospholipid bilayer cellular membrane in a highly distinct manner, which can be relevant for applications that require adhesion, mechanical transduction, or integration.

# 2. EXPERIMENTAL SECTION

2.1. Materials. Gelatin (Type A), methacrylic anhydride, and polyethlyene glycol diacrylate (PEGDA  $-M_n$  700) were purchased from Sigma-Aldrich. The photoinitator used (LAP, lithium phenyl-2,4,6-trimethylbenzoylphosphinate) was purchased from Allevi, Inc., and the visible light used for polymerization was attached to the Allevi 2 bioprinter. All chemicals were of analytical reagent grade and used without further purification.

2.2. Synthesis of the BIL Conjugated GelMA (BioGel) and BIL Conjugated PEGDA (BioPEG). Choline bitartrate and acrylic acid (Sigma-Aldrich) were mixed in a equimolar ratio at 50 °C for 5 h under an inert nitrogen atmosphere to synthesize choline acrylate (BIL) followed by overnight vacuum purification of the product at room temperature.<sup>32</sup> The GelMA polymer was made using a previously described method.<sup>36</sup> A 10% (w/v) gelatin (Sigma-Aldrich) solution and 8 mL of methacrylic anhydride (Sigma-Aldrich) were reacted for 3 h under inert conditions. Unreacted material methacrylic acid was dialyzed for 5 days and frozen at -80 °C for 24 h followed by lyophilization for 5-7 days. Polyethylene glycol (PEGDA) has an average M<sub>n</sub> of 700 (Sigma-Aldrich). GelMA and PEGDA were used to synthesize the bioadhesives, namely, BioGel (25% (w/v) GelMA, 20% (w/v) BIL) and BioPEG (25% (w/v) PEGDA, 20% (w/v) BIL) adhesives. Methacrylated polymer and choline acrylate were mixed in various ratios, and their physical and adhesive characteristics were studied. The adhesive was made from the prepolymer and BIL mixed in varying proportions in distilled water. To the mixtures, 0.5% (w/v) lithium phenyl-2,4,6-trimethylbenzoylphosphinate (LAP) photoinitiator was added; LAP is preferred over other photoinitiators due to its high water solubility and cytocompatibilty.<sup>37</sup> Hydrogels were then

applied and rapidly photo-cross-linked in the presence of visible light in the Allevi 2 bioprinter at a wavelength of 450 nm and intensity of 3 MW/cm<sup>2</sup> for 120 and 60 s for GelMA and PEGDA, respectively.

2.3. <sup>1</sup>H NMR Analysis of Bioadhesives. <sup>1</sup>H NMR was used to characterize the bioadhesive structure. A Varian Inova-500 NMR spectrometer was used. <sup>1</sup>H NMR spectra of choline bitartrate, choline acrylate, GelMA prepolymer, and bioadhesive samples were obtained. The reduction in the rate of C=C methacrylate double bond  $(-\partial(C=C)/\partial t)$  in GelMA was used to understand the cross-linking of the polymer, in addition to bioionic liquid conjugation to polymer.

2.4. Mechanical Properties of the Bioadhesives. Mechanical testing, including calculation of elastic and compressive moduli on each bioadhesive composition, was performed by using an EZ-SX Mechanical tester (Shimadzu). Cylindrical test specimens of diameter 5 mm and height 5 mm were made in polydimethylsiloxane (PDMS) molds. The test specimens were kept in Dulbecco's phosphatebuffered saline (DPBS) for 4 h at 37 °C and allowed to swell prior to testing. For each test, at least five samples were tested.

In the compression tests, the specimens were compressed between two plates at 1 mm/min and the load and strain were recorded. For the tensile tests, the hydrogels were stretched at 1 mm/min until failure. The compression and elastic moduli were calculated as the slope of the linear region of the stress-strain curve. For each test, at least five samples were tested to perform the statistical significance

2.5. In Vitro Degradation Test and Swelling Ratio of the Bioadhesives. BioGel and BioPEG were produced as previously mentioned (Section 2.2). The test was performed based on a previously mentioned method.<sup>32</sup> The samples were lyophilized, weighed, and with 1 mL of DPBS or at 37 °C incubated in a 24 well plate for 2 weeks. The DPBS solutions were replenished every 7 days, at days 1, 7, and 14. The samples were removed and lyophilized for 24 h, and the weight was obtained. Degradation percentage (D%) of the bioadhesive was estimated in terms of the loss of weight. For each test, at least five samples were tested to perform the statistical significance test.

The equilibrium swelling ratios of BioGel and BioPEG adhesives were evaluated using cylinder-shaped adhesives prepared as per the method described for the compression test, and DPBS was used to wash the sample thrice. Then they were freeze-dried to weigh the samples in dry conditions and immersed at 37 °C in DPBS for 2, 4, 6, 8, and 24 h followed by weighing again after immersion. The ratio of the swollen sample mass to lyophilized sample mass was used to compute the swelling ratio and water uptake. For each test, at least five samples were tested to perform the statistical significance test.

2.6. In Vitro Adhesive Properties of the Bioadhesives. Shear strengths of the BioGel and BioPEG adhesives were tested according to the modified ASTM F2255-05 standard for tissue adhesives.<sup>38</sup> A 1 cm × 1 cm layer of gelatin was applied to two 2 cm × 2 cm square pieces, cut from a glass slide. The gelatin layer dried overnight functioned as a base layer. The uncoated area, later used for clamping the glass slide, was covered by tape. 25  $\mu$ L of hydrogel precursor solution was cross-linked between the gelatin coated glass slides, and the slides were then placed in a mechanical tester and pulled apart at a strain rate of 1 mm/min. At the point of detachment, shear strength was calculated for at least five samples for statistically significant results.

Wound closure of the fabricated adhesives was calculated by using the ASTM F2458-05 standard.  $^{39}$  Porcine skin, with excess fat removed, was obtained from a butcher. This was cut into small strips and immersed into PBS to prevent drying prior to testing. The tissue was razor-sliced in the middle to simulate a wound, and to this slit, 100  $\mu$ L of polymer solution was applied and photo-cross-linked using visible light. Maximum adhesive strengths of the samples were obtained at the point of tear, with strain rates of 1 mm/min applied using a mechanical tester. At least five samples were tested per condition to perform the statistical significance test.

Burst pressures of the fabricated adhesives were calculated by using the ASTM F2392-04 standard. <sup>40</sup> A 5 mm × 5 mm puncture was made in the center of 5 cm  $\times$  5 cm skin and was placed in connection from

a custom-built burst pressure apparatus. The apparatus had a pressure meter and a syringe pressure setup. Air was made to flow through at 0.5 mL/s using a syringe pump. The skin was punctured at the puncture covered with the bioadhesives and photo-cross-linked. This was followed by initiating the pump and sensor. Once the hydrogel ruptured, the airflow was stopped and the burst pressure was measured. For each test, at least five samples were tested to perform the statistical significance test.

2.7. Ex Vivo Burst Pressure Measurement of the Bioadhesives. Burst pressures of the fabricated adhesives were calculated by using the ASTM F2392-04 standard. Porcine heart and lung were obtained from a local butcher. A 5 mm × 5 mm puncture was made in the left chamber of the heart, and it was placed in connection from a custom-built burst pressure apparatus. The apparatus consisted of a pressure meter, and air was allowed to flow using at a volumetric rate of 0.5 mL/s. The organ was punctured, covered with bioadhesive, and cross-linked with visible light. The pump and the sensors were then initiated. The burst pressure was computed when the hydrogel ruptured, after which the airflow was terminated. A similar test was carried out for the lung. At least five samples were tested per condition to perform the statistical significance test.

2.8. In Vitro Clotting Study on the Bioadhesives. SEM imaging was performed to analyze the hemostatic property of the engineered adhesive using a method previously described.<sup>41</sup> EDTAanticoagulated whole blood (6 mL) was centrifuged at 2300 rpm for 5 min to prepare the RBC pellet. The plasma and buffy coat layers were discarded. The pellet was washed thrice using 40 mL of isotonic saline (0.9% w/v aqueous NaCl solution, pH 7.4). The oil mixture, consisting of 1 mL, 2.6 parts by weight of benzyl benzoate and 1 part by weight of cottonseed oil, was then added to the RBCs. The oil mixture has a density intermediate to RBCs and the isotonic saline. This oil-RBC suspension was centrifuged for 10 min at 4500 rpm, and supernatant oil was discarded. The thin oil film over the RBC pellet was removed by tapping with cotton, incubated with the adhesive sample overnight at 37 °C, and dehydrated for freeze drying. The lyophilized specimen attached to the SEM stubs were coated with gold/palladium (Au/Pd) prior to SEM imaging, acquired by a Phenom Pure SEM from Nanoscience. The clotting time was measured from RBC coagulation tests on at least five images of five samples using ImageJ software.

**2.9.** In Vitro Biocompatibility of the Bioadhesives. On the surface of adhesive,  $5 \times 10^4$  cells/well were cultured in a 24 well plate with 500  $\mu$ L of DMEM, supplemented with 10% FBS (fetal bovine serum), growth medium. 2D cultures were kept at 37 °C in a 5% CO<sub>2</sub> humidified incubator for 7 days, and the DMEM was replenished after 48 h

The cell viability of primary C2C12 cultured on the surface of BioGel and BioPEG was evaluated by an Invitrogen Live/Dead viability kit, as per manufacturer's instructions. Cells were stained for 15 min at 37 °C with calcein AM (0.5  $\mu$ L/mL) and ethidium homodimer-1 (EthD-1) in DPBS (2  $\mu$ L/mL). Fluorescence images were obtained on days 1, 4, and 7 post-seeding with the Axio Observer Z1 inverted microscope (Zeiss). The number of live/viable and dead cells as green and red spots, respectively, was quantified by ImageJ software, and the cell viability was computed as the ratio of the number of live cells to the total number of cells.

Cell metabolic activity was evaluated at 1, 4, and 7 days by a PrestoBlue assay (Life Technologies). 2D cultures of C2C12 were incubated for 2 h at 37  $^{\circ}\mathrm{C}$  in 500  $\mu\mathrm{L}$  of 10% PrestoBlue growth medium. Resulting fluorescence at 560 (excitation) and 590 nm (emission) was measured with control wells being used to determine the background.

Surface spreading of the cells on the bioadhesive was imaged through fluorescence staining of F-actin filaments and cell nuclei. 2D cultures at days 1, 4, and 7 were incubated for 45 min with Alexa fluor 488 labeled phalloidin (1:1000 in DPBS, Invitrogen). DPBS was used for three consecutive washes, samples were counterstained with 1  $\mu$ L/mL DAPI (4′,6-diamidino-2-phenylindole, Invitrogen) in DPBS for 5

min, and the fluorescence images were acquired with an Axio Observer Z1 inverted microscope.

2.10. In Vivo Biocompatibility and Degradation of the Bioadhesives. All the animal experiments were approved by the ICAUC as per protocol 2018-004, at Rowan SOM. Male Wistar rats weighing 200-250 g were procured from Charles River (Boston, MA, USA). The animals were kept under circadian rhythm conditions at the local animal care facility. 4.0% isoflurane induction and 1-2.5% maintenance were used to induce anesthesia. This was followed by administering 0.02 to 0.05 mg kg<sup>-1</sup> subcutaneous buprenorphine for pain control. On the posterior mediodorsal skin, eight 1 cm incisions were made. Around these incisions, small lateral subcutaneous pockets were made by blunt dissection. 5 mm disks of the bioadhesives were implanted into these pockets. The wound was closed anatomically, and the animals allowed recovery from anesthesia. Animals were euthanized by CO2 asphyxiation after 4, 14, and 28 post-implantations. The samples were retrieved with the associated tissue.

2.11. In Vivo Hemorrhage Study of the Bioadhesives. 2.11.1. Tail Cut Model. One group of eight rats underwent a standardized tail cut technique approved by the Rowan University IACUC and developed by Morgan et al. 42 for the measurement of uncontrolled hemorrhage in rats. All rats were weighed preoperatively. Anesthesia was induced inside an induction chamber with inhaled 4% isoflurane and 100% oxygen followed by a maintenance dose of 1-2% isoflurane delivered via the nose cone. The depth of anesthesia was confirmed by a pedal pinch. Rat tails were marked 4 cm from the tip and transected with a scalpel. The tail stump was immediately placed in a 1.5 mL microcentrifuge tube to collect the shed blood. After 2 min of uncontrolled hemorrhage, 0.8 mL of BioGel was applied to the wound. Of the eight rats, four rats received BioGel and four rats received only the polymer without conjugation of BIL (25% (w/v) GelMA). After an additional 2 min, 0.2 mL of BioGel was applied to the wound. A total of 1.0 mL of BioGel was applied to each wound. Blood loss was recorded in 2 min intervals for the first 14 min of the experiment (2 min before intervention, 2 min during intervention, and 10 min after intervention) followed by 6 min intervals for the next 12 min of the procedure, for a total of 26 min. Blood loss was calculated as a percentage of total blood volume. Total blood volume was calculated using body weight (kg) multiplied by 65 mL/kg, a known ratio of body weight:blood volume in rats. All rats were sacrificed with isoflurane overdose at the conclusion of the 26 min hemodynamic monitoring window, with bilateral thoracotomy as a secondary method of euthanasia.

2.11.2. Liver Wedge Model. One group of 20 rats underwent a standardized liver wedge technique approved by the Rowan University IACUC and developed by Morgan et al.42 for the measurement of uncontrolled hemorrhage in rats. Ten rats received BioGel, five with the unconjugated polymer (25(w/v) % GelMA) and five with the polymer conjugated with BIL (BioGel). Ten rats received BioPEG, five with the unconjugated polymer (25% (w/v) PEGDA) and five with the polymer conjugated with BIL (BioPEG). All rats were weighed preoperatively. Initial anesthesia with inhaled 4% isoflurane and 100% oxygen was used. An esthesia was maintained with 1-2% isoflurane. Rats were placed supine, and their abdomens were shaved and prepped. A 3.0 cm midline laparotomy was performed to expose the abdominal cavity, and the left lobe of the liver was delivered onto the rat abdomen. One  $3.0 \times 1.5$  cm wedge of the left liver lobe was removed to cause the initial liver injury. A preweighed gauze below the liver collected shed blood. After 2 min, 0.5 mL of product was applied to the liver wound. After an additional 2 min, 0.5 mL of product was again applied to the liver wound. The gauze was changed and weighed in 2 min intervals for the first 14 min of the experiment (2 min before intervention, 2 min during intervention, and 10 min after intervention) followed by 6 min intervals for the next 12 min of the procedure, for a total of 26 min. Blood loss was calculated as a percentage of total blood volume. Total blood volume was calculated using body weight (kg) multiplied by 65 mL/kg. All rats were sacrificed with isoflurane overdose at the conclusion of the 26 min hemodynamic monitoring window. Rats

Scheme 1. Synthesis of BIL and Adhesive Hydrogels (BioGel and BioPEG): (a) Acrylation of Choline Bitartrate To Form Choline Acrylate (BIL) and (b) Reaction between GelMA, PEGDA, and Bioionic Liquid To Form BioGel and Bio-PEG

underwent severing of the diaphragm as a secondary method of euthanasia.

#### 3. RESULTS AND DISCUSSION

3.1. Synthesis and Characterization of the Bioionic Liquid and Bioadhesives. The synthesis of BIL and the adhesive is illustrated in Scheme 1. It entails the synthesis of BIL as the first step based on the reaction of choline bitartrate and acrylic acid. The next step entails the conjugation of the synthesized BIL with the polymer (GelMA or PEGDA). The BIL was conjugated with the polymer at concentrations of 0-20% (w/v). The conjugation was carried out by mixing the BIL with a 25% (w/v) solution of GelMA or PEGDA.

The resulting polymer/BIL conjugate was then cross-linked by visible light induced photopolymerization, using LAP as the photoinitiator to form the hemostatic bioadhesives (BioGel and BioPEG). The acrylation of choline bitartrate to make choline acrylate was measured using FTIR, while the conjugation of the BIL to the polymers was measured by <sup>1</sup>H NMR (Figure 1 and Figure S1). In the FTIR, we notice the appearance of a peak at 1720 cm<sup>-1</sup>, which primarily indicates the formation of the ester bond via acrylation.

Similarly, in <sup>1</sup>H NMR, the hydrogen peak of acrylate at 5.9– 6.3 ppm indicates the acrylation of choline bitartrate forming choline acrylate. <sup>1</sup>H NMR spectra also ascertained the conjugation of the BIL to the polymer. Methacrylate groups appear in the conjugated polymer at ~5.7 and ~6.1 ppm, confirming polymer-BIL conjugation. This peak was absent in non-BIL conjugated polymer. The appearance of a sharp peak at  $\delta \sim 3.1-3.2$  ppm in the conjugated polymer corresponds to the three hydrogen atoms of choline (ammonium ion), and this also confirms the conjugation of BIL to the polymer.

3.2. In Vitro Adhesive Properties of the Bioadhesives. Wound closure is associated with tissue stress and damage. In order to mitigate these complications, BioGel- and BioPEGbased adhesive materials could be an alternative strategy. We characterized the in vitro lap shear, adhesive and burst strength tests, and the response to shear, compression, or extension as well as high pressures upon the adherence of the gel to tissue, all in accordance to the ASTM F2255-05 standard 18,38 (Figure 2a). Figure 2b,c shows the shear strengths of BioGel and BioPEG with increasing BIL concentrations. The shear strength of BioGel increased from 109.63 ± 12.42 (GelMA with 0% BIL) to  $359.39 \pm 18.72$  kPa for BioGel with 20% BIL. Similarly, for BioPEG, the shear strength increased from 73.40  $\pm$  3.84 kPa for the polymer with 0% BIL to 241.00  $\pm$  12.09 kPa at 20% BIL.

The shear strengths of BioGel and BioPEG with high BIL concentrations are significantly higher than reported values for commercially available tissue adhesives such as Ethicon's Evicel and Baxter's Coseal, two commercially available adhesives. The shear strengths of Evicel and Coseal (Figure S2) are 207.65  $\pm$ 67.3 and 69.7  $\pm$  20.6 KPa, respectively.

The adhesive strength of BioGel increased from  $0.23 \pm 0.02$ (GelMA with 0% BIL) to  $2.25 \pm 0.02$  kPa for BioGel with 20% BIL concentration (Figure 2d,e). Similarly, for BioPEG, the adhesive strength increased from  $7.01 \pm 0.20$  kPa for the polymer with 0% BIL to  $38.70 \pm 0.30$  kPa at 20% BIL. The adhesive strength of BioPEG with high BIL concentration is significantly higher than BioGel and reported values for commercially available tissue adhesives such as Ethicon's Evicel and Baxter's Coseal. The adhesive strengths of Evicel and Coseal (Figure S2) are  $24.80 \pm 2.51$  and  $26.32 \pm 2.69$  kPa, respectively. 43 The design of polymers for tissue adhesion entails tailoring properties to ensure high tissue adhesion and appropriate mechanical strength. Hydrogel adhesives for soft tissues need mechanical characteristics comparable to native tissue to ensure proper tissue movement. The adhesion properties should be high enough to enable attachment to the surrounding tissues.

The ability of an adhesive to withstand pressure from tissues and fluids under the wound site can be established by the burst pressure test. We tested burst pressure of the fabricated adhesives based on a variation of the ASTM F2392-04 standard testing for surgical sealants. The results are shown in Figure 2f,g. Burst pressures for BioGel and BioPEG at 0% BIL concentration were 9.17  $\pm$  0.66 and 25.60  $\pm$  0.99 kPa, respectively. This subsequently increased to  $101.74 \pm 2.12$  and 69.42 ± 1.59 kPa, respectively, for BioGel and BioPEG at a final BIL concentration of 20%. These values were also significantly higher than that of currently available tissue adhesive.43

We infer from the results that the introduction of BIL functionalization to GelMA or PEGDA improves the adhesion

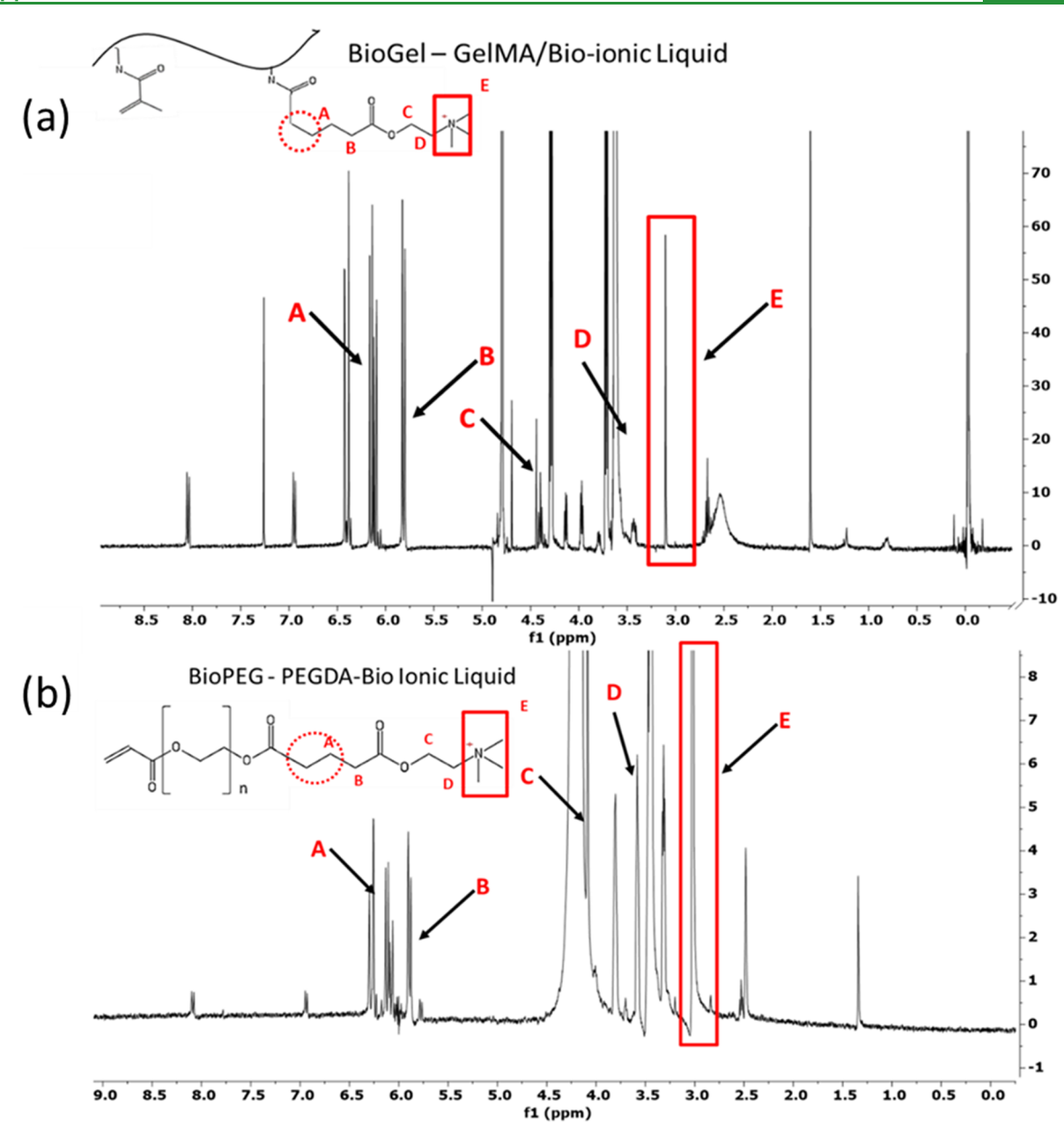


Figure 1. 1H NMR analysis of (a) BioGel and (b) BioPEG. BioGel and BioPEG adhesives were formed by using 0.5% lithium phenyl-2,4,6trimethylbenzoylphosphinate (LAP) at 60 s of light exposure.

of the hydrogel to tissues. The adhesive property is directly related to electrostatic interactions. It is also related to better film-forming properties, which increase with increasing overall molecular weight. The molecular weight, in turn, is dependent on the average molecular mass of repeat units in the polymer, which increases with increasing functionalization by bulky choline pendant groups. Both GelMA and PEGDA on their own are good film formers, and they already have the allowance for polar interactions. 44,45 However, the introduction of BIL-based side groups significantly increases these strong electrostatic interactions leading to high adhesion and shear as well as burst pressure strength. We also expect that the surface BIL heads of the adhesive layer will interact with the phospholipid bilayers of the exposed cells wherein the polar heads may be expected to enhance adhesion.

3.3. In Vitro Hemostatic Properties of the Bioadhe**sive.** The efficacy of biomaterial adherence to wet surfaces can be improved by endowing the material with hemostatic

properties. This property would also allow for reduction of intra- and post-operative tissue blood loss. 40

Although some effective hemostatic materials have been developed, none of the current materials also possess strong adhesive properties. 47–49 We studied the hemostatic properties of BioGel and BioPEG with varying BIL concentrations from 0-20%, and the results are shown in Figure 3 and Figures S6 and S7. The extent and rapidity of clot formation increase significantly with increasing BIL concentration. Even without any BIL functionalization, the clotting time reduced slightly compared to control (Figure 3a,b). The clotting time decreases from  $7.5 \pm 0.50$  to  $4.875 \pm 0.12$  min with 5% BIL polymers. With a BIL concentration of 20%, the clotting time reduces further to  $1.13 \pm 0.13$  min indicating an increase in coagulation efficiency with increasing BIL concentration. Similar results were demonstrated in the case of BioPEG. When the bioadhesive samples were incubated with RBC pellets overnight to perform SEM on the samples (Figure

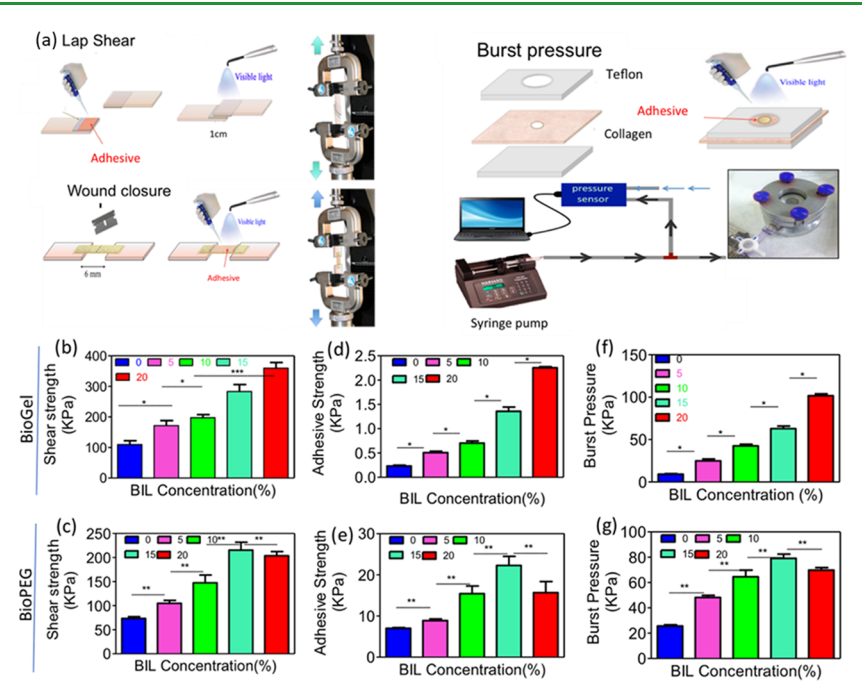


Figure 2. In vitro sealing properties of the BioGel and BioPEG. (a) Schematic diagram of lap shear, wound closure, and burst pressure tests. (b,c) Standard lap shear test was used to determine the sealant's shear strength  $(n \ge 5)$  with different percentages of BIL concentration. (d,e) Standard wound closure of porcine skin was used to test the sealant's adhesion strength  $(n \ge 5)$  with different percentages of BIL concentration. (f,g) Standard burst pressure test was used to evaluate the sealant's burst pressure  $(n \ge 5)$  with different percentages of bioionic liquid (BIL). Data are means ± SD. P values were determined by one-way ANOVA followed by Tukey's multiple comparisons test (\*P < 0.05, \*\*P < 0.01, \*\*\*P < 0.001).

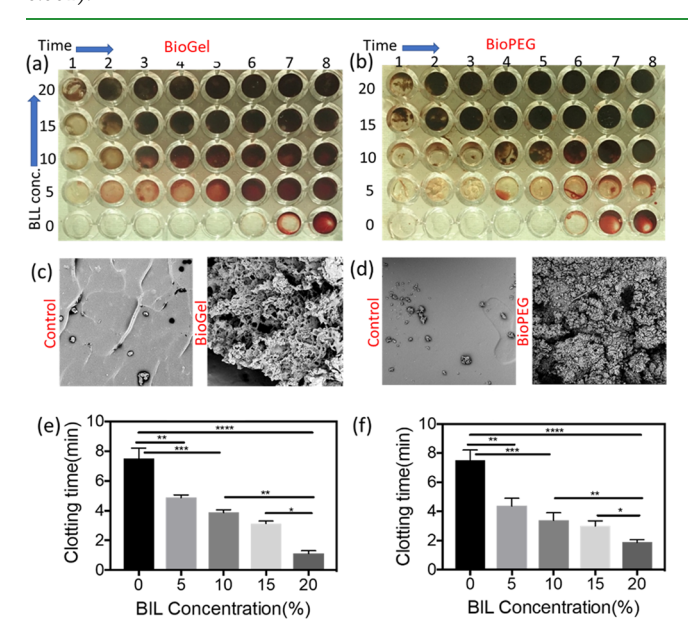


Figure 3. In vitro clotting assay of BioGel and BioPEG. (a,b) Photograph of the well plate based clotting assay with increasing concentration of BIL. SEM of RBC coagulation with (c) control (25% (w/v) GelMA) and BioGel (25% (w/v) GelMA, 20% (w/v) BIL) and (d) control (25% (w/v) PEGDA) and Bio-PEG (25% (w/v) PEGDA, 20% (w/v) BIL). (e,f) Quantification of decrease in clotting time with increasing concentration of bioionic liquid. Data are means ± SD. P values were determined by one-way ANOVA followed by Tukey's multiple comparisons test (\*P < 0.05, \*\*P < 0.01, \*\*\*P < 0.001).

3c,d), the images indicated that, with increasing concentration of the BIL, the coagulation of the RBC's increased. Cell membranes consist of a phospholipid bilayer, of which 1,2dipalmitoyl-glycero-3-phosphatidyl choline (DPPC) is a major constituent.<sup>50</sup> Choline functionalization imparts a quaternary ammonium moiety—the cholinium head group—which, over the mechanism of cellular adhesion, interacts with phosphatidyl choline groups, forming quaternary nitrogen-phosphorus pairs, creating a quadrupole with high electrostatic forces. 41,51

When macromolecules and cellular surfaces interact, the former adsorbs and brings the surfaces into greater proximity in a bridge conformation. Also, the exclusion of glycocalyx from the intercellular space pushes the cells together owing to the osmotic pressure gradient. The same mechanism, when applied to red blood cells, causes their distortion due to overcoming of their elasticity by the adhesive forces. Quaternary nitrogen and phosphorus heads make a dipole and provide binding forces for cellular coagulation and hence hemostasis.<sup>52</sup>

3.4. In Vitro Swelling, Degradation, and Mechanical Properties of the Bioadhesive. The ideal requisites of a bioadhesive would entail its flexibility to match the dynamic environment and movement of native tissues. This requires that the biodegradability be controlled and the metabolites of biodegradation be noncytotoxic. Hydrogels can be metabolized through various pathways—enzymatic degradation or simply via hydrolysis at either acidic or basic pH conditions. 55,56 Also, for the hydrogel to prevent rejection as a foreign invasive object and be eventually metabolized, it must be adequately hydrated via body fluids. However, excessive water uptake and degradation could lead to impaired mechanical and adhesive properties. Thus, water uptake and swelling for a tissue adhesive must be optimized to suit the in vivo conditions and the intended application. The swelling and degradation are shown in Figure S3. The swelling of BioGel versus the polymer/BIL concentration is shown in Figure S3b.

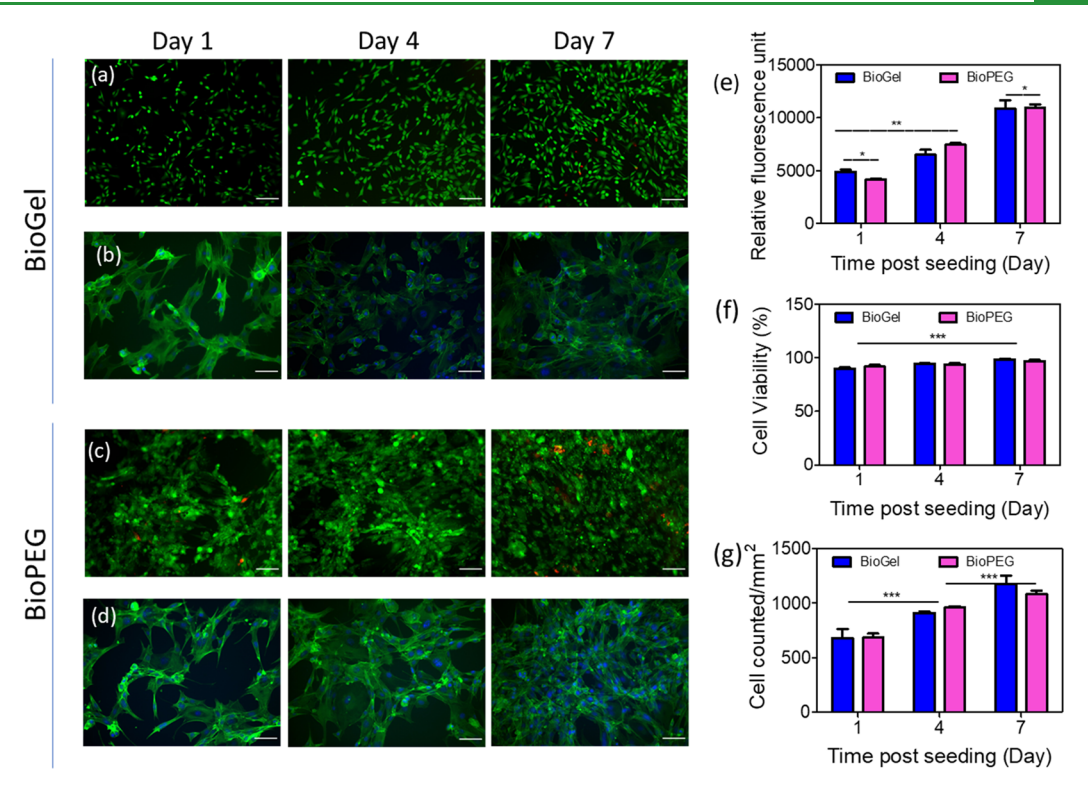


Figure 4. In vitro biocompatibilities of BioGel and BioPEG. Representative live/dead images and F-actin/DAPI fluorescent images at days 1, 4, and 7 post-seeding of (a,b) BioGel and (c,d) BioPEG. (e) Quantification of metabolic activity, relative fluorescence units (RFU), using PrestoBlue assay. (f) Quantification of cell viability of live/dead images. (g) Quantification of cell proliferation based on DAPI-stained cell nuclei. Data are means  $\pm$  SD. P values were determined by one-way ANOVA followed by Tukey's multiple comparisons test (\*P < 0.05, \*\*P < 0.01, \*\*\*P < 0.001).

Irrespective of the BIL concentration, BioGel grew to ∼120% of the swelling ratio. For the GelMA (0% BIL), there is a steady increase in the water uptake and swelling with time, while with BIL concentrations of 5, 10, 15, and 20%, there is an initial gradual water uptake followed by a sudden increase to reach 120% after 24 h. This effect is progressively more pronounced with increasing BIL concentration, indicating that BILs can expedite degradation without significant differences in swelling after 24 h. A similar trend was seen with BIL incorporated PEGDA (BioPEG). With 0% BIL incorporation, the polymers swelled much faster. With increasing BIL incorporation, the swelling rate decreased due to initial intrinsic physical cross-linking induced by electrostatic interactions mediated by the BIL functional groups. The final swelling achieved for the PEGDA-backbone-based BioPEG polymers was ~40% lower than that for GelMA-based polymers due to the intrinsic nature of the PEGDA backbone, which has lower hydrophilic affinity than GelMA.

As the polymer absorbs water, in a semidilute solution, polymer chain conformations form overlapping correlation blobs with hydration spheres around each blob dictated by functional groups with water affinity. For GelMA, this is relatively straightforward; with no functionalization, the semidilute regime blobs slowly open up in a favorable solvent and allow more and more water in until the cross-link conformation resists any further expansion. With BIL functionalization, there is an increased strong interaction between monomers inside a single correlation blob, as well as between the monomers in the periphery of the correlation blob, which act as additional physical cross-links conferring an initial resistance to polymer expansion with hydration. This

situation needs to be slowly broken by hydrating the hydrophilic groups intrinsically in the GelMA- and BILfunctionalized BioGel. Hence, the rate at which the water expands the gel is slower in functionalized BioGel rather than in GelMA. However, since the GelMA is already highly hydrophilic, the addition and variation of BIL concentration do little to alter that. Considering that these are chemically crosslinked to the same extent using LAP, hence, the final expansion of such a polymer would eventually be arrested by the existence of those chemical cross-links acting as ultimate tethers. Thus, for polymers, the density of cross-linking determines the final swelling, and hence, the polymers swell to a limited and similar ultimate extent.<sup>57</sup> This is a desirable property when designing an adhesive formulation wherein the material must swell and mimic in vivo conditions but not to the extent that it starts to disintegrate and defeat the primary mechanical requirement of usage.

In vitro degradation tests can simulate the in vivo behavior of hydrogels when exposed to physiological conditions. Si Since the compounds are organic in nature, the degradation products of these polymers are expected to be noncytotoxic. Degradation studies show in Figure S3e that, for BioGel with a BIL concentration of 0%, the degradation increases from 8.5% at day 1 to 12.3% at day 14, with the degradation tapering after 7 days. There is a general increase in the amount of degradation at day 1, day 7, and day 14 with an increase in the concentration of BIL. For 5% BIL concentration, the degradation increases from 13% at day 1 to around 18% at the end of day 7, tapering off at 19% at day 14. The degradation for 20% BIL in polymer is 19% at day 1 and increases to 24.6% on day 14. While the trend of degradation is

the same, it may be observed that there are greater levels of degradation with an increase in BIL concentration. It is possible for the quaternary ammonium head in choline to act as a catalyst along with the water of hydration to cause hydrolysis of the many integrated functionalities in both the GelMA and PEGDA backbone hence degrading it, thus increasing degradation with BIL concentration in the polymer. Degradation follows the same trend in both GelMA- and PEGDA-based polymers, but the lower water uptake in PEGDA results in an intrinsically lower extent of degradation.

Mechanical properties of the bioadhesives were characterized through tensile and compression tests. The elastic moduli obtained from tensile tests are shown in Figure S3d,h. Tensile tests on BioGel and BioPEG hydrogels show that the elastic moduli (Figure S3d,h) and compression moduli (Figure S2c,g) of the bioadhesives could be modulated by varying the percentage of BIL. As a general trend, the mechanical properties increase with the increase in BIL concentration. With 0% BIL, the compression modulus is  $37.79 \pm 0.47$  kPa and the tensile modulus is  $202.83 \pm 1.26$  kPa. These values increase to  $186.46 \pm 7.51$  and  $355.36 \pm 18.25$  kPa, respectively, for BioGel with 20% BIL concentration. Similarly, BioPEG with 0% BIL (PEGDA) shows a compression modulus of 26.12 ± 2.63 kPa and a tensile modulus of  $102.93 \pm 1.61$  kPa, which increase to 212.15  $\pm$  13.11 and  $361.21 \pm 7.25$  kPa, respectively, at 20% BIL concentration in

Hydrogels exhibit a tradeoff between stiffness and flexibility to resist shear, tension, or compression forces while maintaining structural integrity. The increase in compressive strength and tensile modulus of the polymers with BIL over unfunctionalized GelMA or PEGDA can be attributed to an increase in the intensity of electrostatic interactions. The attachment of the bulky choline group as side chains to the GelMA or PEGDA structure makes the backbone stiff hence increasing the respective moduli. Enhanced mechanical properties are also a result of an increase in the overall repeat unit molecular weight due to bulky choline side chains. The polar and hydrogen bond interactions also increase significantly with BIL functionalization. These strong electrostatic interactions obstruct the uncoiling and slipping of chains and result in the BIL groups acting as a physical cross-link, tethering the structure together.

3.5. Cell Viability, Proliferation, and Metabolic **Activity on the Bioadhesive.** To investigate the biocompatibilities of BioGel and BioPEG, the in vitro live/dead assay was performed. The assay determined the viability of C2C12 cells on the BioGel and BioPEG surfaces over a period of 7 days. Cell attachment and spreading on hydrogels were evaluated through F-actin/DAPI (Figure 4) immunofluorescence staining. The results indicate (Figure 4f,g) that the viabilities of seeded cells on day 7 were 98.5  $\pm$  0.5 and 97  $\pm$ 1.0% for BioGel and BioPEG, respectively. Cells seeded on the surfaces of BioGel and BioPEG exhibit similar viabilities at day 1 post-seeding. The metabolic activity was quantified by the PrestoBlue assay and was shown (Figure 4 e) to increase significantly during the period of cell culture from 4910.80 ± 180.13 to 10847.71  $\pm$  797.17 RFU for BioGel and 4170.60  $\pm$ 90.25 to 10954.80  $\pm$  299.44 RFU for BioPEG. These results underscore the potential of the bioadhesive as a biocompatible sealant material capable of promoting cell adhesion, growth, and proliferation.

3.6. In Vivo Biocompatibility of the Bioadhesive. The in vivo degradation of BioGel and BioPEG synthesized was evaluated after subcutaneous implantation into rats (Figure 5a,b). Samples were explanted on days 4, 14, and 28 to study

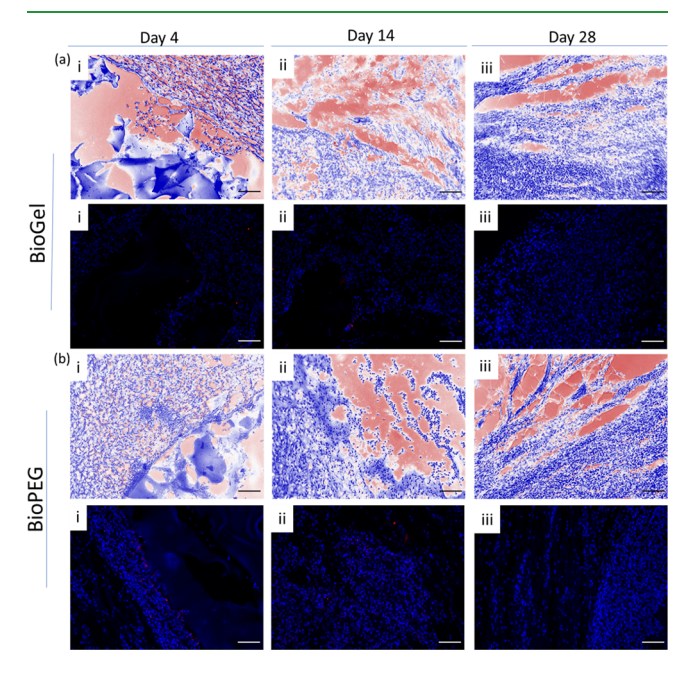


Figure 5. In vivo compatibility of bioadhesive. Hematoxylin and eosin (H&E) staining and fluorescence immunohistochemical analysis of macrophages (CD68) of (a) BioGel and (b) BioPEG explanted with surrounding tissue after (i) 4, (ii) 14, and (iii) 28 days of implantation, counterstained with nuclei (DAPI).

the compatibility and degradation. In vivo degradation and morphological changes were characterized by hematoxylin and eosin (H&E) staining; the staining indicates the presence of the hydrogel until day 4 (Figure 5a-i,b-i), and the tissue architecture revealed that there is no significant macrophage infiltration implying that the bioadhesives cause less or no adverse inflammatory responses compared to GelMA or PEGDA. The degradation rate of the sealant must be appropriate to ensure that the sealant does not degrade completely prior to tissue healing. 12,59 Fluorescence immunohistological staining for macrophages (CD68) was used to characterize the local immune response. CD68 macrophage invasion and infiltration, at the adhesive-subcutaneous tissue interface, were observed at day 4 but not at day 28. This observation suggested that the CD68 cells are able to infiltrate the implant and may control the degradation through enzymatic hydrolysis of the hydrogel matrix.

3.7. Ex Vivo and in Vivo Performance of the Bioadhesive. To characterize the properties of the bioadhesives, burst pressure measurement was carried out on the explanted porcine heart and lung (Figure 6a-e). The specimen chamber was pressurized by pumping in phosphate-buffered saline under a constant flow rate, while the pressure was recorded with a pressure gauge. GelMA exhibited a burst pressure value of  $9.33 \pm 1.20$  kPa, which increased 10-fold with increasing concentration of BIL to 100.00 ± 2.89 kPa for BioGel. Similarly, the difference between PEGDA and BioPEG increased from  $7.33 \pm 1.45$  to  $61.66 \pm 6.01$  kPa, respectively.

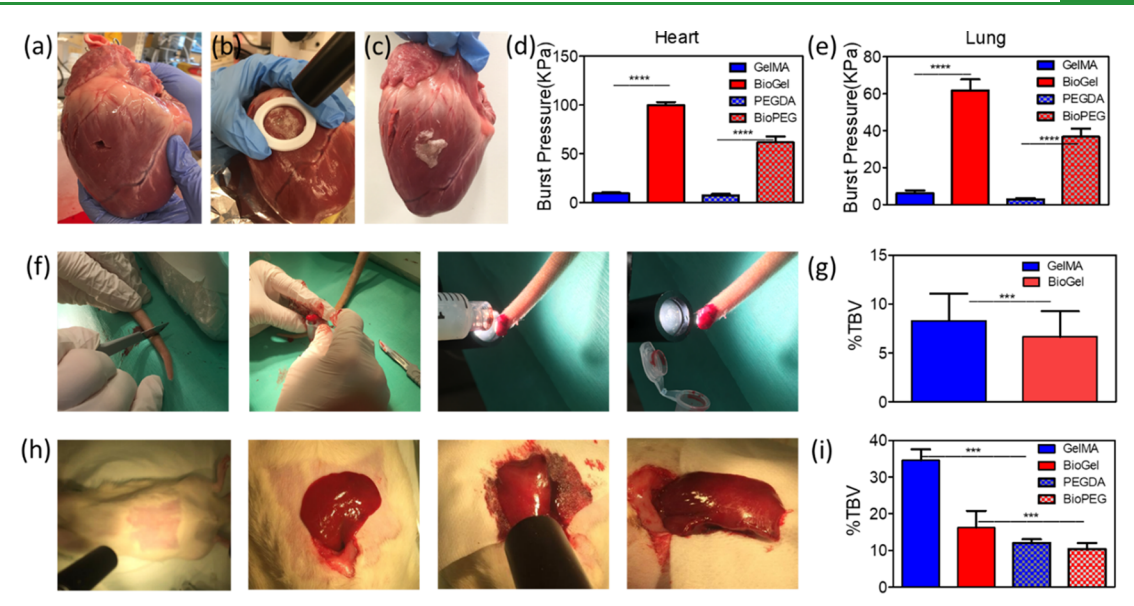
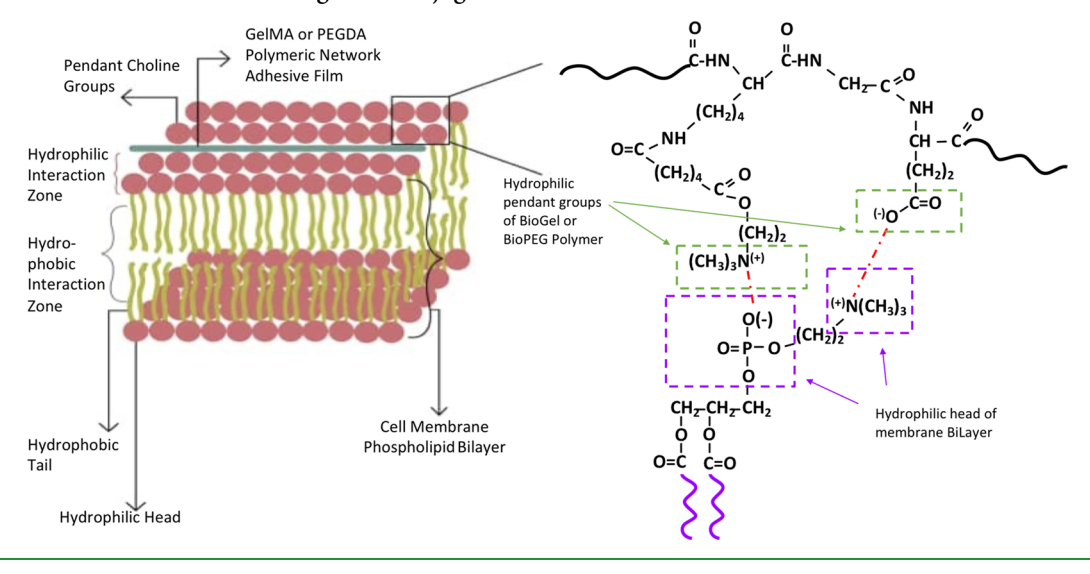


Figure 6. Ex vivo and in vivo performance characterization of the bioadhesives. (a) Puncture, (b) sealing, and (c) patching of the wound in porcine heart. (d,e) Burst pressure measurement in explanted heart and lung comparing GelMA and PEGDA with BioGel and BioPEG. (f,g) In vivo tail cut model was performed to estimate the loss in % total blood volume (TBV). Control value is from ref 42. (h,i) Liver laceration model was performed to estimate the %TBV comparing GelMA and PEGDA with BioGel and BioPEG. Data are means ± SD. P values were determined by one-way ANOVA (\*P < 0.05, \*\*P < 0.01, \*\*\*P < 0).

Scheme 2. Bioadhesion Mechanism Using BIL Conjugation to Biomaterials



These results corroborated that BioGel and BioPEG sealants have significantly greater sealing abilities than previously reported clinically available sealant materials and sutures. 43

Functional evaluation of BioGel and BioPEG was conducted in a rat model of class I hemorrhage (the tail cut) and class II hemorrhage (the liver wedge resection) (Figure 6f-i). When we performed the tail cut model with GelMA and BioGel, the mean losses of TBV were  $8.27 \pm 2.77$  and  $6.64 \pm 2.62\%$ , respectively. Previously reported controls note a mean TBV loss of 15.4%. Both GelMA and BioGel effectively inhibit bleeding. 42 Moreover, while GelMA bled continuously until the end of the experiment, BioGel fully stopped blood loss within 2 min. Thus, BioGel is suitable to treat lacerations causing class I hemorrhage. To estimate the ability of the bioadhesive to treat class II hemorrhage, we performed a liver wedge resection with GelMA and BioGel. The mean losses of TBV were  $34.5 \pm 2.9$  and  $16.2 \pm 4.6\%$ , respectively. Previously

reported controls note a mean TBV loss of 19.8%. Both GelMA and BioGel effectively stop bleeding. Most of the bleeding occurred in the first 2 min but continued steadily until the 6 min point. In BioGel after the 7th min, the bleeding stopped completely. The mean losses of TBV were 12.06  $\pm$ 0.98 and 9.282 ± 1.522% for PEGDA and BioPEG, respectively, indicating that with the conjugation of the BIL the bleeding can be retracted. Blood loss was noticeably reduced after application and polymerization of both compounds.

The decrease in the rate of blood loss is reinforced by the substantial decrease in percent total blood volume lost between the experimental animals and the controls. The liver wedge resection model was designed to reproduce class II hemorrhage in rats. The wedge resection performed in that study limited the raw surface of liver resected for bleeding. By making only one incision to remove a piece of the liver edge,

the surface area exposed for bleeding was minimized. In order to challenge the hemostatic properties of the experimental compounds, a more extensive liver wedge resection was performed. We excised a 1.5 cm × 3 cm piece of the liver, creating a right angle to maximize the surface area of bleeding liver tissue. This more extensive resection leads to a percent total blood loss of 48.72% in the control rat, which would qualify as class IV hemorrhage (percent total blood loss >40%). Class IV hemorrhage leads to profound hemodynamic instability in humans and almost always requires operative intervention for bleeding cessation. Both BioGel and BioPEG were able to successfully stopped bleeding from the liver wedge resection. The ability of the compounds to ensure hemostasis in a class IV hemorrhage wound solidifies their reliability as hemostatic agents.

We have demonstrated a new technology platform to develop efficient hemostatic and biocompatible tissue adhesives using conjugation of a choline-based BIL to polymer structures. Two polymer families were studied, which demonstrated significant enhancement in mechanical, adhesion, and hemostatic efficacy with BIL functionalization, likely achieved by hydrophobic interactions with the cellular membrane. Hydrophilic heads and hydrophobic heads bunch together to form a part of the bilayer cellular membrane. 50,53,60 The phosphatidyl choline groups stabilize the cellular membrane bilayer via steric effects and net charge neutrality, preventing it from binding to immunological protein oligomers. 41,51,54,61,62 The mechanism of adhesion with the BIL-modified GelMA and PEGDA polymers can be visualized via the formation of the strong, electrostatically bound quadruple as depicted. At the extracellular surface, the adhesion comprises the interaction between the hydrophobic phosphatidyl choline heads and the choline pendant groups and unreacted carboxyl pendants of the BioGel structure as illustrated in Scheme 2. The two electrostatically bound couples are (1) the negatively charged phosphatidyl group with a positively charged cholinium ion from the BioGel pendant and (2) the cholinium head of the phospatidyl choline and carboxyl anion pendants from the BioGel polymer. These pairs form a tightly bound quadruple with high adhesion propensity. In the BioPEG structure, electrostatic interactions between pendant cholinium groups and phosphatidyl heads of the cell bilayer maintain high levels of adhesion.

Macromolecules cause cellular surface aggregations through adsorptive bridging conformations. The membrane glycocalyx is thought to exclude them from the intercellular space causing an osmotic-gradient-mediated aggregation of cell.<sup>63</sup> The Suo moto action of a macromolecule in cellular aggregation may be enhanced with the BIL-functionalization-mediated adhesive action. As the BIL concentration increases, the adhesive interaction becomes stronger. This has been seen in the choline phosphate density on carrier polymers with cellular aggregation by Yu et al. leading to cellular aggregation and close proximity juxtaposition of membranes.<sup>41</sup> The illustrated general mechanism encompasses the interactions on the outer surface of the membrane bilayer.

# 4. CONCLUSIONS

We present a general biopolymer modification platform for making polymeric tissue adhesives via the incorporation of the BIL functionality in a macromolecule, which will induce a strong electrostatic interaction due to the cholinium moieties with the hydrophilic cellular bilayer heads. The development of this general platform, for converting suitable polymer backbones with the appropriate usage of BIL, is expected to allow for the rapid and vast development of biocompatible adhesives, tunable to the property requirement of a given tissue. The adhesives discussed here with the two polymer families as examples provide a proof of concept with their hemostatic ability and in vivo compatibility, allowing for wider vistas of applicability opening up possibilities for enhancing the robustness of surgical and in-field application. This development not only offers adhesive and hemostatic adhesive properties but also potentially opens up vistas for other advantages such as mechano-transduction.

## ASSOCIATED CONTENT

# S Supporting Information

The Supporting Information is available free of charge on the ACS Publications website at DOI: 10.1021/acsami.9b08757.

<sup>1</sup>H NMR analysis of acrylate; FTIR of choline bitartrate; standard lap shear rate; standard pressure test; degradation profiles and swelling ratios; setup for measuring in vitro adhesive properties; performance of composites; clotting assay; effect of pH on in vitro adhesive and swelling performance (PDF)

## AUTHOR INFORMATION

# **Corresponding Author**

\*E-mail: noshadi@rowan.edu.

#### ORCID ®

Vaishali Krishnadoss: 0000-0002-0015-1824 Iman Noshadi: 0000-0002-0683-5426

## **Author Contributions**

The manuscript was written through contributions of all authors. All authors have given approval to the final version of the manuscript.

#### **Funding**

The authors are grateful for financial support from Rowan University Startup fund and NSF 1919092 award.

The authors declare no competing financial interest.

#### **REFERENCES**

- (1) Prausnitz, M. R.; Langer, R. Transdermal Drug Delivery. Nat. Biotechnol. 2008, 26, 1261.
- (2) Li, J.; Mooney, D. J. Designing Hydrogels for Controlled Drug Delivery. Nat. Rev. Mater. 2016, 1, 16071.
- (3) Duflo, S.; Thibeault, S. L.; Li, W.; Shu, X. Z.; Prestwich, G. D. Vocal Fold Tissue Repair in Vivo Using a Synthetic Extracellular Matrix. Tissue Eng. 2006, 12, 2171-2180.
- (4) Sharma, B.; Fermanian, S.; Gibson, M.; Unterman, S.; Herzka, D. A.; Cascio, B.; Coburn, J.; Hui, A. Y.; Marcus, N.; Gold, G. E.; Elisseeff, J. H. Human Cartilage Repair with a Photoreactive Adhesive-Hydrogel Composite. Sci. Transl. Med. 2013, 5, 167ra6.
- (5) Grinstaff, M. W. Designing Hydrogel Adhesives for Corneal Wound Repair. Biomaterials 2007, 28, 5205-5214.
- (6) Ghobril, C.; Charoen, K.; Rodriguez, E. K.; Nazarian, A.; Grinstaff, M. W. A Dendritic Thioester Hydrogel Based on Thiolthioester Exchange as a Dissolvable Sealant System for Wound Closure. Angew. Chem., Int. Ed. 2013, 52, 14070-14074.
- (7) Roche, E. T.; Wohlfarth, R.; Overvelde, J. T. B.; Vasilyev, N. V.; Pigula, F. A.; Mooney, D. J.; Bertoldi, K.; Walsh, C. J. A Bioinspired Soft Actuated Material. Adv. Mater. 2014, 26, 1200-1206.
- (8) Feiner, R.; Engel, L.; Fleischer, S.; Malki, M.; Gal, I.; Shapira, A.; Shacham-Diamand, Y.; Dvir, T. Engineered Hybrid Cardiac Patches

- with Multifunctional Electronics for Online Monitoring and Regulation of Tissue Function. *Nat. Mater.* **2016**, *15*, 679.
- (9) Annabi, N.; Tamayol, A.; Shin, S. R.; Ghaemmaghami, A. M.; Peppas, N. A.; Khademhosseini, A. Surgical Materials: Current Challenges and Nano-enabled Solutions. *Nano Today* **2014**, *9*, 574–589.
- (10) Ferreira, P.; Pereira, R.; Coelho, J. F. J.; Silva, A. F. M.; Gil, M. H. Modification of the Biopolymer Castor Oil with Free Isocyanate Groups to be Applied as Bioadhesive. *Int. J. Biol. Macromol.* **2007**, *40*, 144–152.
- (11) de Oliveira, C. L.; dos Santos, C. H. M.; Bezerra, F. M. M.; Bezerra, M. M.; de Lima Rodrigues, L. Utilização de Adesivos de Cianoacrilatos em Suturas de Pele. *Rev. Bras. Cir. Pläst.* **2010**, 25, 573.
- (12) Annabi, N.; Yue, K.; Tamayol, A.; Khademhosseini, A. Elastic Sealants for Surgical Applications. *Eur. J. Pharm. Biopharm.* **2015**, 95, 27–39.
- (13) Duarte, A. P.; Coelho, J. F.; Bordado, J. C.; Cidade, M. T.; Gil, M. H. Surgical Adhesives: Systematic Review of the Main Types and Development Forecast. *Prog. Polym. Sci.* **2012**, *37*, 1031–1050.
- (14) Bouten, P. J. M.; Zonjee, M.; Bender, J.; Yauw, S. T. K.; van Goor, H.; van Hest, J. C. M.; Hoogenboom, R. The Chemistry of Tissue Adhesive Materials. *Prog. Polym. Sci.* **2014**, *39*, 1375–1405.
- (15) Singer, A. J.; Quinn, J. V.; Hollander, J. E. The Cyanoacrylate Topical Skin Adhesives. Am. J. Emerg. Med. 2008, 26, 490–496.
- (16) Singer, A. J.; Thode, H. C., Jr A Review of the Literature on Octylcyanoacrylate Tissue Adhesive. *Am. J. Surg.* **2004**, *187*, 238–248.
- (17) Montanaro, L.; Arciola, C. R.; Cenni, E.; Ciapetti, G.; Savioli, F.; Filippini, F.; Barsanti, L. A. Cytotoxicity, Blood Compatibility and Antimicrobial Activity of Two Cyanoacrylate Glues for Surgical Use. *Biomaterials* **2000**, *22*, 59–66.
- (18) Sierra, D. H.; Feldman, D. S.; Saltz, R.; Huang, S. A Method to Determine Shear Adhesive Strength of Fibrin Sealants. *J. Appl. Biomater.* **1992**, *3*, 147–151.
- (19) Kajiwara, K.; Osada, Y. Gels Handbook; Academic Press, 2000.
- (20) Belcher, E.; Dusmet, M.; Jordan, S.; Ladas, G.; Lim, E.; Goldstraw, P. A Prospective, Randomized Trial Comparing BioGlue and Vivostat for the Control of Alveolar Air Leak. *J. Thorac. Cardiovasc. Surg.* **2010**, *140*, 32–38.
- (21) Hill, A.; Estridge, T. D.; Maroney, M.; Monnet, E.; Egbert, B.; Cruise, G.; Coker, G. T. *J. Biomed. Mater. Res., Part A* **2001**, *58*, 308–312
- (22) Bhagat, V.; Becker, M. L. Degradable Adhesives for Surgery and Tissue Engineering. *Biomacromolecules* **2017**, *18*, 3009–3039.
- (23) Pascual, G.; Sotomayor, S.; Rodríguez, M.; Pérez-Köhler, B.; Kühnhardt, A.; Fernändez-Gutiérrez, M.; San Romän, J.; Bellón, J. M. Cytotoxicity of Cyanoacrylate-Based Tissue Adhesives and Short-Term Preclinical In Vivo Biocompatibility in Abdominal Hernia Repair. *PLoS One* **2016**, *11*, e0157920.
- (24) Spotnitz, W. D. Fibrin Sealant: Past, Present, and Future: A Brief Review. *World J. Surg.* **2010**, 34, 632–634.
- (25) Mehdizadeh, M.; Yang, J. Design Strategies and Applications of Tissue Bioadhesives. *Macromol. Biosci.* **2013**, *13*, 271–288.
- (26) Liu, Q.-P.; Hou, X.-D.; Li, N.; Zong, M.-H. Ionic liquids from Renewable Biomaterials: Synthesis, Characterization and Application in the Pretreatment of Biomass. *Green Chem.* **2012**, *14*, 304–307.
- (27) Fukaya, Y.; Iizuka, Y.; Sekikawa, K.; Ohno, H. Bio Ionic Liquids: Room Temperature Ionic Liquids Composed Wholly of Biomaterials. *Green Chem.* **2007**, *9*, 1155–1157.
- (28) Fukumoto, K.; Yoshizawa, M.; Ohno, H. Room Temperature Ionic Liquids from 20 Natural Amino Acids. *J. Am. Chem. Soc.* **2005**, 127, 2398–2399.
- (29) Bagno, A.; D'Amico, F.; Saielli, G. Computing the H NMR Spectrum of a Bulk Ionic Liquid from Snapshots of Car–Parrinello Molecular Dynamics Simulations. *ChemPhysChem* **2007**, *8*, 873–881.
- (30) Egorova, K. S.; Gordeev, E. G.; Ananikov, V. P. Biological Activity of Ionic Liquids and Their Application in Pharmaceutics and Medicine. *Chem. Rev.* **2017**, *117*, 7132–7189.
- (31) Kumar, P. K.; Bisht, M.; Venkatesu, P.; Bahadur, I.; Ebenso, E. E. Exploring the Effect of Choline-Based Ionic Liquids on the Stability

- and Activity of Stem Bromelain. J. Phys. Chem. B 2018, 122, 10435-10444.
- (32) Noshadi, I.; Walker, B. W.; Portillo-Lara, R.; Shirzaei Sani, E.; Gomes, N.; Aziziyan, M. R.; Annabi, N. Engineering Biodegradable and Biocompatible Bio-ionic Liquid Conjugated Hydrogels with Tunable Conductivity and Mechanical Properties. *Sci. Rep.* **2017**, *7*, 4345
- (33) Blusztajn, J. K. Choline, a Vital Amine. Science **1998**, 281, 794–795.
- (34) Zeisel, S. H. Choline: an Essential Nutrient for Humans. *Nutrition* **2000**, *16*, 669–671.
- (35) Yue, B.; Pattison, E.; Roberts, W. L.; Rockwood, A. L.; Danne, O.; Lueders, C.; Möckel, M. Choline in Whole Blood and Plasma: Sample Preparation and Stability. *Clin. Chem.* **2008**, *54*, 590–593.
- (36) Yue, K.; Trujillo-de Santiago, G.; Alvarez, M. M.; Tamayol, A.; Annabi, N.; Khademhosseini, A. Synthesis, Properties, and Biomedical Applications of Gelatin Methacryloyl (GelMA) Hydrogels. *Biomaterials* **2015**, *73*, 254–271.
- (37) Fairbanks, B. D.; Schwartz, M. P.; Bowman, C. N.; Anseth, K. S. Photoinitiated Polymerization of PEG-diacrylate with Lithium phenyl-2,4,6-trimethylbenzoylphosphinate: Polymerization Rate and Cytocompatibility. *Biomaterials* **2009**, *30*, 6702–6707.
- (38) ASTM F2255-05. Standard Test Method for Strength Properties of Tissue Adhesives in Lap-Shear by Tension Loading; ASTM International, 2015; 13 (1).
- (39) ASTM F2458-05. Standard Test Method for Wound Closure Strength of Tissue Adhesives and Sealants; ASTM International, 2015; 13 (1).
- (40) ASTM F2392-04. Standard Test Method for Burst Strength of Surgical Sealants; ASTM International, 2015; 13 (1).
- (41) Yu, X.; Liu, Z.; Janzen, J.; Chafeeva, I.; Horte, S.; Chen, W.; Kainthan, R. K.; Kizhakkedathu, J. N.; Brooks, D. E. Polyvalent Choline Phosphate as a Universal Biomembrane Adhesive. *Nat. Mater.* **2012**, *11*, 468.
- (42) Morgan, C. E.; Prakash, V. S.; Vercammen, J. M.; Pritts, T.; Kibbe, M. R. Development and Validation of 4 Different Rat Models of Uncontrolled Hemorrhage. *JAMA Surg.* **2015**, *150*, 316–324.
- (43) Annabi, N.; Rana, D.; Shirzaei Sani, E.; Portillo-Lara, R.; Gifford, J. L.; Fares, M. M.; Mithieux, S. M.; Weiss, A. S. Engineering a Sprayable and Elastic Hydrogel Adhesive with Antimicrobial Properties for Wound Healing. *Biomaterials* **2017**, *139*, 229–243.
- (44) Bigi, A.; Cojazzi, G.; Panzavolta, S.; Rubini, K.; Roveri, N. Mechanical and Thermal Properties of Gelatin Films at Different Degrees of Glutaraldehyde Crosslinking. *Biomaterials* **2001**, 22, 763–768
- (45) Priola, A.; Gozzelino, G.; Ferrero, F.; Malucelli, G. Properties of Polymeric Films Obtained from u.v. Cured Poly(ethylene glycol) diacrylates. *Polymer* **1993**, *34*, 3653–3657.
- (46) Behrens, A. M.; Sikorski, M. J.; Kofinas, P. Hemostatic Strategies for Traumatic and Surgical Bleeding. *J. Biomed. Mater. Res. Part A* **2014**, *102*, 4182–4194.
- (47) Behrens, A. M.; Sikorski, M. J.; Li, T.; Wu, Z. J.; Griffith, B. P.; Kofinas, P. Blood-Aggregating Hydrogel Particles for Use as a Hemostatic Agent. *Acta Biomater.* **2014**, *10*, 701–708.
- (48) Gaharwar, A. K.; Avery, R. K.; Assmann, A.; Paul, A.; McKinley, G. H.; Khademhosseini, A.; Olsen, B. D. Shear-Thinning Nanocomposite Hydrogels for the Treatment of Hemorrhage. *ACS Nano* **2014**, *8*, 9833–9842.
- (49) Hangge, P.; Stone, J.; Albadawi, H.; Zhang, Y. S.; Khademhosseini, A.; Oklu, R. Hemostasis and Nanotechnology. *Cardiovasc. Diagn.Ther.* **2017**, *7*, S267–S275.
- (50) Singer, S. J.; Nicolson, G. L. The Fluid Mosaic Model of the Structure of Cell Membranes. *Science* **1972**, *175*, 720–731.
- (51) Hazen, S. L.; Chisolm, G. M. Oxidized Phosphatidylcholines: Pattern Recognition Ligands for Multiple Pathways of the Innate Immune Response. *Proc. Natl. Acad. Sci. U. S. A.* **2002**, *99*, 12515–12517.
- (52) Burdge, G. C.; Kelly, F. J.; Postle, A. D. Synthesis of Phosphatidylcholine in Guinea-Pig Fetal Lung involves Acyl

- Remodelling and Differential Turnover of Individual Molecular Species. *Biochim. Biophys. Acta, Lipids Lipid Metab.* **1993**, *1166*, 251–257.
- (53) Sohlenkamp, C.; López-Lara, I. M.; Geiger, O. Biosynthesis of Phosphatidylcholine in Bacteria. *Prog. Lipid Res.* **2003**, *42*, 115–162. (54) Goldfine, H. Bacterial Membranes and Lipid Packing Theory. *J. Lipid Res.* **1984**, *25*, 1501–7.
- (55) Zhao, X.; Sun, X.; Yildirimer, L.; Lang, Q.; Lin, Z. Y.; Zheng, R.; Zhang, Y.; Cui, W.; Annabi, N.; Khademhosseini, A. Cell Infiltrative Hydrogel Fibrous Scaffolds for Accelerated Wound Healing. *Acta Biomater.* **2017**, *49*, 66–77.
- (56) El-Sherbiny, I. M.; Yacoub, M. H. Hydrogel Scaffolds for Tissue Engineering: Progress and Challenges. *Global Cardiology Sci.Pract.* **2013**, 2013, 38.
- (57) Ganji, F.; Vasheghani, F. S.; Vasheghani, F. E. Theoretical Description of Hydrogel Swelling: A Review. *Iran. Polym. J.* **2010**, *19*, 375–398
- (58) Kharkar, P. M.; Kiick, K. L.; Kloxin, A. M. Designing Degradable Hydrogels for Orthogonal Control of Cell Microenvironments. *Chem. Soc. Rev.* **2013**, *42*, 7335–7372.
- (59) Annabi, N.; Zhang, Y.-N.; Assmann, A.; Sani, E. S.; Cheng, G.; Lassaletta, A. D.; Vegh, A.; Dehghani, B.; Ruiz-Esparza, G. U.; Wang, X.; Gangadharan, S.; Weiss, A. S.; Khademhosseini, A. Engineering a Highly Elastic Human Protein—based Sealant for Surgical Applications. Sci. Transl. Med. 2017, 9, eaai7466.
- (60) Doherty, G. J.; McMahon, H. T. Mediation, Modulation, and Consequences of Membrane-Cytoskeleton Interactions. *Annu. Rev. Biophys.* **2008**, *37*, 65–95.
- (61) Peschel, A.; Jack, R. W.; Otto, M.; Collins, L. V.; Staubitz, P.; Nicholson, G.; Kalbacher, H.; Nieuwenhuizen, W. F.; Jung, G.; Tarkowski, A.; van Kessel, K. P. M.; van Strijp, J. A. G. Staphylococcus aureus Resistance to Human Defensins and Evasion of Neutrophil Killing via the Novel Virulence Factor MprF is Based on Modification of Membrane Lipids with l-lysine. *J Exp. Med.* 2001, 193, 1067–1076.
- (62) Brooks, D. E. Mechanism of Red Cell Aggregation. *Blood Cells, Rheology and Aging*; Springer: Berlin, Heidelberg, 1988; 158–162.
- (63) Neu, B.; Meiselman, H. J. Depletion-mediated Red Blood Cell Aggregation in Polymer Solutions. *Biophys. J.* **2002**, *83*, 2482–2490.